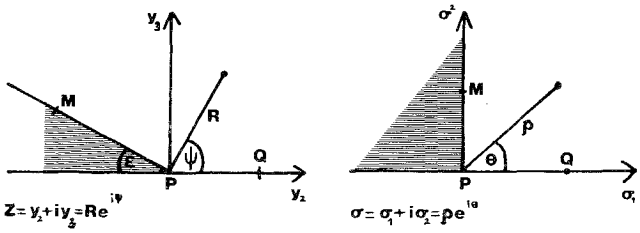

Fig. 2 Mapping of the trailing-edge region.

along the wing ($\psi=\pi-\omega$). From these two equations, we eliminate the constant $Bc^{2/k}$ to calculate Φ_P.

Further terms could be incorporated into Eqs. (5) and (6) to obtain a higher-order solution, in which case Eq. (7) would have to be applied at additional grid points to eliminate the extra constants introduced.

Concluding Remarks

The use of a coordinate system, which has already been successfully used in the computation of transonic flows past swept wings, has been shown to give rise to a singular term in the equation of motion at a sharp swept trailing edge. An alternative to the present approach using a local solution appears to be to calculate the potential at the trailing edge by extrapolation along the wing surface (see Forsey and Carr[4]). However, the linear extrapolation used assumes that the potential has a linear behavior in ξ^3, a quality which it can be shown not to possess. In addition, the equation of motion is not satisfied at the trailing edge in that case.

How sensitive the calculated flow is to differences in the numerical treatment at the trailing edge is open to conjecture, but it seems worthwhile to draw the attention of other investigators to a possible source of error, and to suggest a way of avoiding it.

Acknowledgment

Thanks are due to the Science Research Council for financial support during the period that the author was at the University of Southampton, and to K. W. Mangler and J. H. B. Smith for their helpful comments.

References

[1] Duck, P. W., "The Numerical Calculation of Steady Inviscid Supercritical Flow Past Ellipsoids without Circulation," Aeronautical Research Council, U.K., R&M 3794, 1977.

[2] Jameson, A., "Iterative Solution of Transonic Flows over Airfoils and Wings, Including Flows at Mach 1," *Communication on Pure and Applied Mathematics*, Vol. 27, May 1974, pp. 283-309.

[3] Clapworthy, G. J., "Subcritical Flow without Circulation Past a Swept Semi-Infinite Elliptic Cylinder," *Aeronautical Quarterly*, Vol. 28, Pt. 2, May 1977, pp. 142-148.

[4] Forsey, C. and Carr, M. P., A.R.A. Tech. Memo. (to appear).

[5] Clapworthy, G. J., "Flow Near the Trailing Edge of a Swept Wing," Polytechnic of North London, Tech. Rept. PNL-MA-20, 1978.

Modes of Turbulent Vortex Shedding from a Pipe-Jet System in a Cross-Flow

John W. Trischka*
Syracuse University, Syracuse, N.Y.

I. Introduction

A PAPER by Moussa, et al[1] showed the characteristics of vortex shedding from a pipe-jet system in a cross-flow. The emphasis was on shedding from the jet. A few downstream measurements made at vertical positions above and below the plane of the pipe orifice led to the conclusion that the pipe and jet constituted a single shedding system. In other experiments, this system was broken into two isolated parts by means of a flat plate placed in the plane of the orifice, and vortex shedding occurred independently from the jet and from the pipe.

This Note presents the results of more extensive measurements of the unified pipe-jet system in which no plate was used in the plane of the pipe orifice. It has been found that the pipe and jet shed vortices at significantly different rates. The differences depend on the ratio of jet speed U_j to the speed of the undisturbed cross-flow U_∞. The existence of two different shedding systems for the jet and for the pipe has led to naming them the "jet mode" and the "pipe mode," respectively.

When observations were made by varying only the z coordinate parallel to the pipe axis, it was found that in the jet region far above the pipe orifice there was only one shedding frequency, that of the jet mode. Similarly, for positions well below the pipe orifice only the frequency of the pipe mode was found. However, for several pipe diameters above and below the orifice, two shedding frequencies were observed; Fig. 1 is an example. One of these frequencies is identical with that of the pipe mode; the other identical with that of the jet mode. In the range in which frequencies are observed, the modes are said to "overlap."

Measurements made over the full range of the z coordinate from pipe base to jet locations at which shedding disappeared, and over a wide range of U_j/U_∞, showed that four different modes could be defined. Each mode overlapped the z-adjacent mode. The jet and pipe modes occur distinguishably for $U_j/U_\infty > 5$. For $U_j/U_\infty < 1$, a weak jet condition, there is no discernible jet mode, but because of the importance of the end effect, the end of the pipe from the lip to a distance several diameters below the lip sheds vortices at a slower rate than the main body of the pipe. This new mode is called the "end mode." The fourth mode, called the "base mode," overlaps the pipe mode and occurs in the region where the pipe meets the floor of the wind tunnel. The shedding frequency of the base mode is lower than that of the pipe mode.

II. Apparatus and Measurements

The apparatus has been described in detail in Ref. 1. The wind tunnel has a cross section 1.22 m high by 0.61 m wide. A perpendicular pipe, $D=2.54$ cm o.d. and 2.36 cm i.d., comes through the tunnel floor to a height of 46 cm. A turbulent jet issues from the open end of the pipe. A speed-sensing hot wire probe is connected to an anemometer circuit whose output passes through a linearizer to a narrow band, real-time spectrum analyzer. This, in turn, drives an x-y recorder after an averaging time of 5 min has elapsed. The incremental fre-

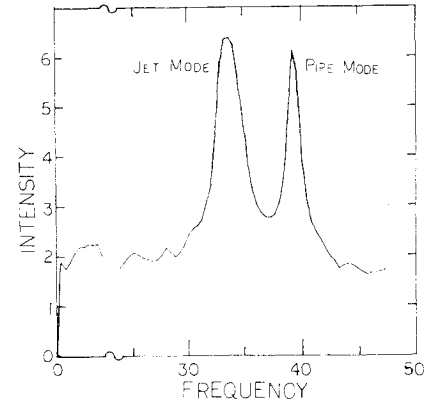

Fig. 1 Typical trace of power spectrum showing jet mode, pipe mode, and a reference turbulence level near zero frequency. The intensity scale is abitrary.

Received Oct. 2, 1978.

Index category: Jets, Wakes, and Viscid-Inviscid Flow Interactions.

*Professor of Physics, Dept. of Physics.

quency change of the analyzer is in 0.4 Hz steps and the bandwidth of its filters is 0.6 Hz. The right-hand coordinates specifying the hot wire position relative to the center of the pipe exit are x in the downstream direction; y in the cross-stream direction; and z in the vertical pipe axis direction, positive upward. Measurements were made in the range $5<x/D<14.5$ and $-2\leq y/D\leq 2$. The studies of the relationships between the pipe mode and the end mode and between the pipe mode and the jet mode were made in the vertical range from $z/D=-4$ to positive values at which shedding disappeared.

III. Results

Figure 1 is a typical power spectrum for a probe position at which the pipe mode and the jet mode overlap. The higher frequency is that of the pipe mode. For this spectrum $U_j/U_\infty=6.7$, $z/D=-0.7$, $x/D=3.5$ and $y/D=-0.7$. At the left in Fig. 1 a small section, starting at zero frequency, shows the intensity of the turbulent background.

Because of the small differences in Strouhal numbers for different shedding modes, the most reliable and consistent way of presenting results is the use of the dimensionless ratio, which is the difference of the two shedding frequencies, Δf, divided by the mean of these two frequencies, f_m. This ratio is plotted vs U_j/U_∞ in Fig. 2. Data were taken for several values of the Reynolds number, based on the pipe outer diameter. The fractional frequency difference between the end and pipe modes is clearly defined in the range $0.3<U_j/U_\infty<1$. This range is shown with better definition in Fig. 3. The range of clearly defined pipe mode and jet mode differences is $5<U_j/U_\infty<15$. The noticeable effect of Reynolds number is delineated by curves drawn for the same Reynolds number R_∞. It is seen that the frequency difference at a given U_j/U_∞ increases with Reynolds number. In the transitional range $1<U_j/U_\infty<5$, the very small frequency differences are distinctly observable at $R_\infty=13{,}000$. However, if present, they are not observable at $R_\infty=8000$ because of inadequate resolution of separate spectral lines at the low-shedding frequencies. Because of the scatter of the data, no curve was drawn to show the shape in this range. The scatter in the results in Fig. 2 for $U_j/U_\infty>6$ comes principally from the jet mode.

A number of measurements made to establish and verify the existence of the base mode gave a value of $\Delta f/f_m=0.12\pm0.02$. The base-mode frequency is lower than that of the pipe mode.

The Strouhal number for the pipe mode for $2.5<U_j/U_\infty<15$ was 0.200 ± 0.003. In the range of $U_j/U_\infty<2.5$, the Strouhal number of the pipe mode steadily decreased until, at $U_j/U_\infty=0.35$, it was 0.190.

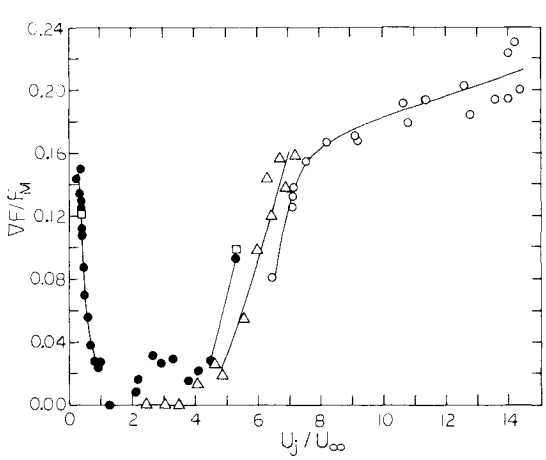

Fig. 2 Fractional frequency difference between modes vs ratio of jet speed U_j to undisturbed tunnel speed U_∞: ●, $R_\infty=13{,}000$; □, $R_\infty=10{,}000$; Δ, $R_\infty=8000$; ○, $R_\infty=4000$.

IV. Discussion

The present measurements show that in the range of U_j/U_∞ studied the vortices shed from a pipe-jet system in a crossflow are characterized by four different overlapping modes, here named the base mode, the pipe mode, end mode, and jet mode. For a very long pipe, the Strouhal number of the pipe mode should be independent of U_j/U_∞. The observed decrease of the Strouhal number of the pipe mode for $U_j/U_\infty<2.5$ can be explained by the extension of the end mode down the pipe as U_j/U_∞ decreases. Consequently, the length of the pipe responsible for the pipe mode decreases and the aspect ratio becomes less and less favorable for true two-dimensional flow.

At the Reynolds numbers in these experiments, the Strouhal number for an infinitely long pipe, according to the Roshko[3] formula, should be 0.212. The lower values found in the present experiments are probably a result of an insufficient aspect ratio at all values of U_j/U_∞.

In order to understand the widths of the spectral peaks of shedding in Fig. 1, the widths being much larger than the bandwidth of the spectrum analyzer, two models were considered. In the first, it was assumed that shedding occurred in bursts of sharply defined frequencies but with different frequencies for different bursts. The second model assumed aperiodic shedding, the time interval between vortices varying randomly. To test these models, runs were made for the minimum averaging time possible, 2.5 s. The spectra consisted of groups of peaks, each much narrower than those observed with the usual 5-min averaging time. These results favor the first model.

The results for the strongly three-dimensional flow of the present system resemble in some respect those found by Gaster[2] for a tapered circular cylinder in a crossflow. He reported several over-lapping modes or "cells," all of which had frequencies less than the Roshko[3] frequency. Along his pipe, for several diameters after it enters his wind tunnel, he reports a shedding mode corresponding to what has been called here the base mode. If the next mode farther along the pipe is considered a body mode, then his value for $\Delta f/f_m$ of about 0.16, is very close to the 0.12 found in the present measurements.

The existence of the base mode, probably caused by the boundary layer at the tunnel wall, makes questionable the arguments that the effective length of a pipe is doubled by reflection in the tunnel wall.

That the shedding frequency of the end mode is lower than that of the pipe mode is qualitatively consistent with the observations on a yawed circular cylinder by Van Atta,[4] who found that the shedding frequency decreased with the yaw angle. An angle of yaw of about 30 deg gave a decrease comparable to the maximum decrease observed in the present experiments.

Etzold and Fiedler[5] reported on the wake structure of a cantilevered, solid cylinder in a crossflow. This is equivalent to $U_j=0$ in the present experiments. Details of measurements made by the present author for $U_j/U_\infty<0.35$ were not

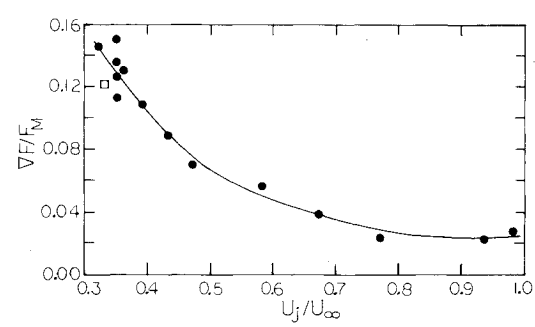

Fig. 3 Fractional frequency difference between the end mode and the pipe mode vs ratio of jet speed U_j to undisturbed tunnel speed U_∞: ●, $R_\infty=13{,}000$; □, $R_\infty=10{,}000$.

reported previously because of difficulties in measuring U_j at the required low speeds. However, spectral lines corresponding to an end mode were found for all jet speeds down to and including $U_j = 0$. Flow visualization experiments at $U_j = 0$ demonstrated the existence of a wake "bubble" at the end of the pipe similar to that found by Etzold and Fiedler (1976) for a solid cylinder.

V. Acknowledgment

The authors thanks S. Eskinazi of the Syracuse University Mechanical and Aerospace Engineering Department for helpful discussions.

References

[1]Moussa, Z. M., Trischka, J. W., and Eskinazi, S., "The Near Field in the Mixing of a Round Jet with a Cross-Stream," *Journal of Fluid Mechanics*, Vol. 80, 1977, p. 49.

[2]Gaster, M., "Vortex Shedding from Circular Cylinders at Low Reynolds Numbers," *Journal of Fluid Mechanics*, Vol. 46, 1971, p. 749.

[3]Roshko, A., "On the Development of Turbulent Wakes from Vortex Streets," NACA Rept. 1191, 1954.

[4]Van Atta, C. W., "Experiments on Vortex Shedding from Yawed Circular Cylinders," *AIAA Journal*, Vol. 6, 1968, p. 931.

[5]Etzold, F. and Fiedler, H., "The Near-Wake Structure of a Cantilevered Cylinder in a Cross-Flow," *Z. Flugwiss*, Vol. 24, 1976, p. 77.

Remarks on Dusty Hypersonic Wedge Flow

Ronald M. Barron* and J. Thomas Wiley†
University of Windsor, Windsor, Ontario, Canada

Introduction

THE study of the motion of solid particles in a dusty gas in the inviscid hypersonic shock layer of a slender wedge was initiated by Probstein and Fassio.[1] Their analysis was developed so as to determine the dust particle trajectories and the collection efficiency for the wedge. Peddieson and Lyu[2] extended their analysis to obtain closed-form solutions for the particle density and temperature distribution. In this Note we propose an alternate approach to the work of Ref. 2. In particular, we derive simpler formulas that allow an examination of the limiting behavior of the particle streamlines and density. We also give a simple physical interpretation related to the collection efficiency of the wedge and correct some results found in Ref. 2.

Analysis and Solution

We employ the notation of Ref. 2 and write the equations governing the dust cloud on a thin wedge in hypersonic flow as

$$(\rho_p u_p)_{,x} + (\rho_p v_p)_{,y} = 0 \tag{1a}$$

$$u_p u_{p,x} + v_p u_{p,y} = \alpha_1 |(u-u_p)^2 + (v-v_p)^2|^{(1-b)/2}(u-u_p) \tag{1b}$$

$$u_p v_{p,x} + v_p v_{p,y} = \alpha_1 |(u-u_p)^2 + (v-v_p)^2|^{(1-b)/2}(v-v_p) \tag{1c}$$

$$u_p T_{p,x} + v_p T_{p,y} = \alpha_2 (T - T_p) \tag{1d}$$

This formulation permits three interphase drag laws,[1] corresponding to low ($b=1$), intermediate ($b=3/5$), and high ($b=0$), Reynolds number ranges.

Equation (1a) implies the existence of a particle streamfunction ψ_p defined by

$$\psi_{p,x} = -\rho_p v_p, \quad \psi_{p,y} = \rho_p u_p \tag{2}$$

Assuming that the clean gas is unaffected by the presence of the dust particles, we have

$$u = 1, \quad v = 0, \quad T = T_s \tag{3}$$

where T_s is the constant temperature of the gas in the shock layer. A von Mises transformation from coordinates (x,y) to (x,ψ_p) transforms the system of Eqs. (1) [using Eqs. (3)] to

$$(\rho_p u_p)_{,x} + \rho_p^2 (u_p v_{p,\psi_p} - v_p u_{p,\psi_p}) = 0 \tag{4a}$$

$$u_p u_{p,x} = \alpha_1 |(1-u_p)^2 + v_p^2|^{(1-b)/2}(1-u_p) \tag{4b}$$

$$u_p v_{p,x} = -\alpha_1 |(1-u_p)^2 + v_p^2|^{(1-b)/2} v_p \tag{4c}$$

$$u_p T_{p,x} = \alpha_2 (T_s - T_p) \tag{4d}$$

In addition, the equation for the particle paths is

$$\frac{dy}{dx} = \frac{v_p}{u_p} \tag{5}$$

Initial conditions associated with the system of Eqs. (4) and (5) are obtained from the shock relations as

$$u_p = 1, \ v_p = -\theta_w, \ T_p = 1, \ y = x_s(\theta_s - \theta_w), \ \rho_p = 1 \text{ at } x = x_s \tag{6}$$

where x_s is the point where the particle streamline along which the integration is being performed meets the shock wave.

Equations (4) and (5) can be solved subject to conditions (6) to obtain the variation of u_p, v_p, T_p, ρ_p, and y along the streamlines. For all values of b, we find

$$u_p = 1 \tag{7}$$

$$T_p = T_s - (T_s - 1)\exp[\alpha_2 (x_s - x)] \tag{8}$$

The solution for the other variables depend on b.

$b=1$:

$$v_p = -\theta_w \exp[\alpha_1 (x_s - x)] \tag{9a}$$

$$y = x_s(\theta_s - \theta_w) + (\theta_w/\alpha_1)\{\exp[\alpha_1 (x_s - x)] - 1\} \tag{9b}$$

$$\rho_p = [1 + (\theta_w/\theta_s)\{\exp[\alpha_1 (x_s - x)] - 1\}]^{-1} \tag{9c}$$

$b=3/5$:

$$v_p = -\theta_w [1 + (2\alpha_1/5)(-\theta_w)^{2/5}(x - x_s)]^{-5/2} \tag{10a}$$

$$y = x_s(\theta_s - \theta_w) - 5\theta_w^{3/5}/(3\alpha_1)\{1 - [1 + (2\alpha_1/5)(-\theta_w)^{2/5}(x - x_s)]^{-3/2}\} \tag{10b}$$

$$\rho_p = [1 + (\theta_w/\theta_s)\{[1 + (2\alpha_1/5)\theta_w^{2/5}(x - x_s)]^{-5/2} - 1\}]^{-1} \tag{10c}$$

Received Oct. 4, 1978.

Index categories: Multiphase Flows; Supersonic and Hypersonic Flow.

*Assistant Professor, Dept. of Mathematics. Member AIAA.

†Graduate Student, Dept. of Mathematics.